EPJ Web of Conferences **86**, 00057 (2015)
DOI: 10.1051/epjconf/ 20158600057

Fusion Hindrance and Quadrupole Collectivity in Collisions of A≃50 Nuclei: The Case of ^{48}Ti + ^{58}Fe

A. M. Stefanini[1,a], G. Montagnoli[2], L. Corradi[1], S. Courtin[3], D. Bourgin[3], E. Fioretto[1], A. Goasduff[4], J. Grebosz[5], F. Haas[3], M. Mazzocco[2], T. Mijatović[6], D. Montanari[2], C. Parascandolo[2], F. Scarlassara[2], E. Strano[2], S. Szilner[6], N.Toniolo[1], and D. Torresi[2]

[1] *INFN, Laboratori Nazionali di Legnaro, I-35020 Legnaro (Padova), Italy*
[2] *Dipartimento di Fisica e Astronomia, Università di Padova, and INFN, Sezione di Padova, I-35131 Padova, Italy*
[3] *IPHC, CNRS-IN2P3, Université de Strasbourg, F-67037 Strasbourg Cedex 2, France*
[4] *CSNSM, CNRS/IN2P3 and Université Paris-Sud, F-91405 Orsay Campus, France*
[5] *Institute of Nuclear Physics, Polish Academy of Sciences, PL 31-342 Cracow, Poland*
[6] *Ruđer Bošković Institute, HR-10002 Zagreb, Croatia*

Abstract. The fusion excitation function of ^{48}Ti + ^{58}Fe has been measured in a wide energy range around the Coulomb barrier, covering 6 orders of magnitude of the cross sections. We present here the preliminary results of this experiment, and a full comparison with the near-by system ^{58}Ni + ^{54}Fe where evidence of fusion hindrance shows up at relatively high cross sections. The sub-barrier cross sections of ^{48}Ti + ^{58}Fe are much larger than those of ^{58}Ni + ^{54}Fe. Significant differences are also observed in the logarithmic derivatives, astrophysical S-factors and fusion barrier distributions. The influence of low-energy nuclear structure on all these trends is pointed out and commented. Coupled-channels calculations using a Woods-Saxon potential are able to reproduce the experimental results for ^{48}Ti + ^{58}Fe. The logarithmic derivative of the excitation function is very nicely fit, and no evidence of hindrance is observed down to around 1 μb. The fusion barrier distribution is rather wide, flat and structureless. It is only in qualitative agreement with the calculated distribution.

1 Introduction

In the collision of two heavy ions at energies near and below the Coulomb barrier, couplings of the relative motion of the two nuclei to their low-energy surface vibrations and/or stable deformations [1, 2] determine the cross sections. Nucleon transfer channels play a concurring role in several cases, and the bare ion-ion potential is important as well. Multi-phonon excitations have been shown [3] to become dominant for medium-heavy nuclei and produce complex fusion barrier distributions, possibly with discrete structures [4, 5]. Below the lower energy limit of such distributions, it has been shown in recent years [6, 7] that fusion excitation functions show a sharp decrease with decreasing energy, well below the expectations based on standard coupled-channels (CC) calculations.

It has been suggested that fusion hindrance is a consequence of the saturation properties of nuclear matter [8], that inhibit a large overlap of the colliding nuclei. In this sense, it should be a general phenomenon in heavy-ion fusion. However, its energy threshold strongly depends on the structure of the colliding nuclei, being in general lower for soft systems, whose barrier distribution may extend to lower energies and thereby "counterbalancing" hindrance, with respect to rigid or closed-shell nuclei. This was observed, e.g., in the comparison of ^{58}Ni + ^{58}Ni with ^{64}Ni + ^{64}Ni [9]. In the A = 40-60 mass range, a few systems were investigated at LNL in recent years (the Ca+Ca systems [10], ^{36}S + ^{48}Ca [11], ^{58}Ni + ^{54}Fe [12]). All of them involve closed-shell nuclei, and show hindrance with different strengths and features. The case of ^{32}S + ^{48}Ca [13] is different: no hindrance effect has been observed down to the sub-μb cross section level. Actually, the rather strong quadrupole mode of ^{32}S, together with positive Q-value transfer couplings, may be responsible for this behavior.

Collective vibrations are known in several nuclei in the mass region A≃40-50, although not so strong as around A≃100. We felt appropriate, therefore, to investigate a case involving such nuclei, because fusion between nuclei with well-known collective excitations at low energies may help clarifying the influence of such inelastic states on fusion and understanding the physics underlying deep sub-barrier fusion.

The system ^{48}Ti + ^{58}Fe is appealing in this sense, since both nuclei have a low-lying quadrupole excitation: the 2^+ states lie at ≈800-900 keV only, while the octupole states are rather high. The behavior of this system will immediately be contrasted with the results obtained for the near-by case ^{58}Ni + ^{54}Fe [12] (closed-shell nuclei), where the hindrance effect is very clear and sets in at the level of the relatively large cross section of ∼200 μb. As a matter of

[a] e-mail: alberto.stefanini@lnl.infn.it

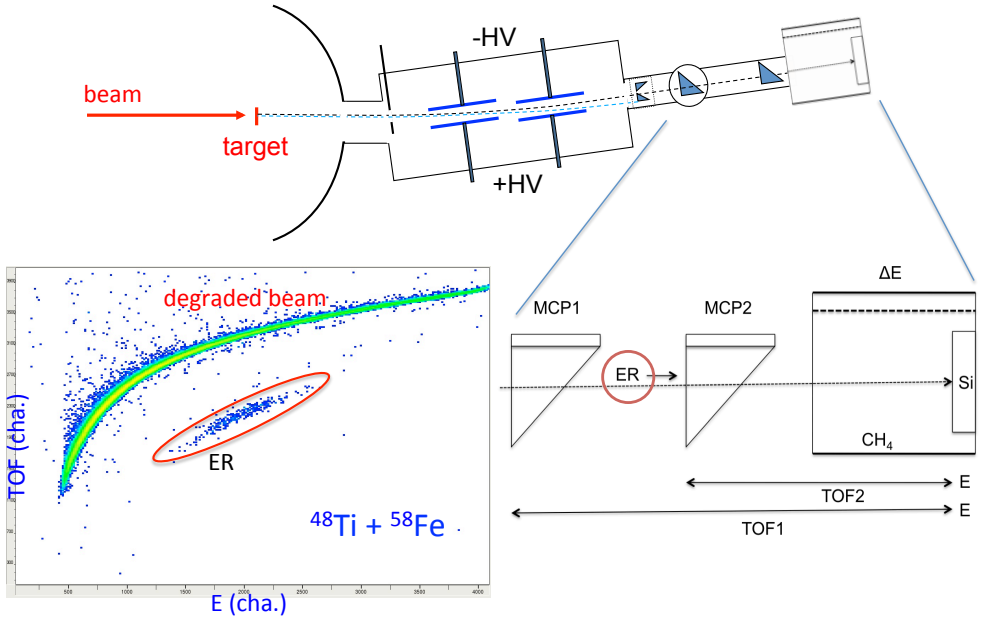

Figure 1. Sketch of the experimental set-up used for the measurement of fusion-evaporation residues (ER) of ^{48}Ti + ^{58}Fe. The matrix is one of the E-ToF spectra obtained during the runs (see text).

fact, it was observed that the cross sections of ^{58}Ni + ^{54}Fe decrease very steeply at the lowest energies, and the logarithmic slope of the excitation function keeps increasing, reaches and overcomes the value L_{CS} expected for a constant astrophysical S factor. Consequently, this shows a clear maximum as a function of the energy.

2 Experiment and Results

The experiment has been performed using the ^{48}Ti beam from the XTU Tandem accelerator of the Laboratori Nazionali di Legnaro of INFN, at energies ranging from 119 MeV to 150 MeV, with intensities around 10 pnA. The targets were 50μg/cm^2 metallic iron evaporations, on a 15μg/cm^2 carbon layer, isotopically enriched to 99.915% in mass 58. The fusion-evaporation residues (ER) were detected by a double Time-of-Flight ΔE-Energy telescope following an electrostatic beam deflector at 0° and at small angles. A more detailed description of the experimental set-up and of the procedures can be found in recent papers [5, 13]. The set-up is schematically shown in Fig. 1, together with one of the Energy-Time-of-Flight two-dimensional spectra obtained at E_{lab}= 125 MeV ($\sigma_{fus} \simeq$700 μb). This shows the clear separation we obtain between ER and beam-like particles. The spectrum was accumulated in around 2 hours of beam time, and it contains ~300 ER.

Beam control and normalization between the different runs were ensured by four collimated silicon detectors placed symmetrically around the beam direction at θ_{lab}= 16°. ER angular distributions were measured at two energies near the Coulomb barrier, 127 and 141 MeV, in order to determine the ratio between the differential ER cross sections and the total, angle-integrated fusion (fusion-fission is negligible for the present system in the measured energy range). No significant variation with energy of the width of the angular distribution, could be noticed.

The absolute cross section scale is estimated to be accurate within ±7%, but statistical uncertainties are much smaller, apart from the very low-energy points. These statistical (relative) errors determine the accuracy of the fusion barrier distribution extracted from the data. We point out, however, that the cross sections presented in this work should be considered preliminary, because the data analysis is still in progress.

The measured excitation function is reported in Fig. 2 (top panel). It is plotted vs. the energy difference from the Coulomb barrier produced by the potential used in the CC calculations discussed in the next Section. In the same figure, also the published cross sections for ^{58}Ni + ^{54}Fe [12] are shown in the corresponding energy scale. This allows us to notice immediately the large enhancement of ^{48}Ti + ^{58}Fe fusion with respect to the other, more stiff, system, in the sub-barrier region. The bottom panel of Fig. 2 shows the same data in a linear energy scale.

3 Coupled-channels Analysis

We have compared the measured cross sections with standard CC calculations performed with the CCFULL [14] code using the Woods-Saxon geometry for the nuclear potential. The Akyüz-Winther potential [15] (AW) has been employed, whose parameters have been slightly modified (keeping the diffuseness unchanged) to match the excitation function in the barrier region. They are V_o= 80.5

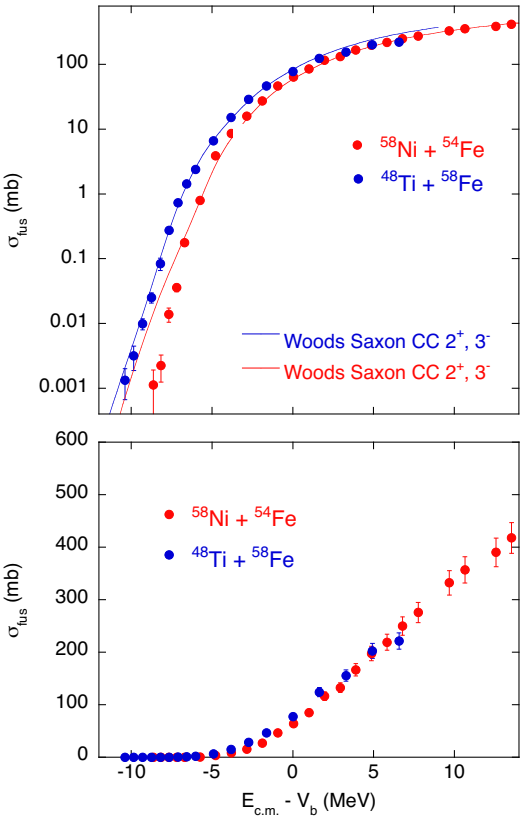

Figure 2. (top) Fusion excitation function of ^{48}Ti + ^{58}Fe measured in the present work (preliminary data, see text), compared to the existing data on ^{58}Ni + ^{54}Fe [12], and to the CC calculations described in the text. (bottom) The same experimental cross sections in a linear scale. The errors are statistical ones in the top panel, and absolute ones in the bottom panel.

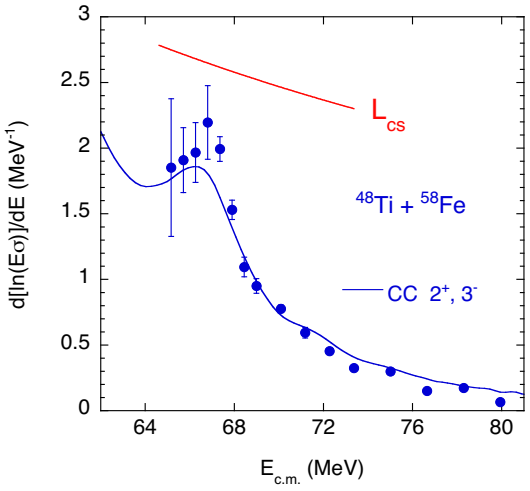

Figure 3. Logarithmic derivative of the excitation function of ^{48}Ti + ^{58}Fe, compared to the CC calculation. L_{CS} is the slope expected for a constant astrophysical S factor.

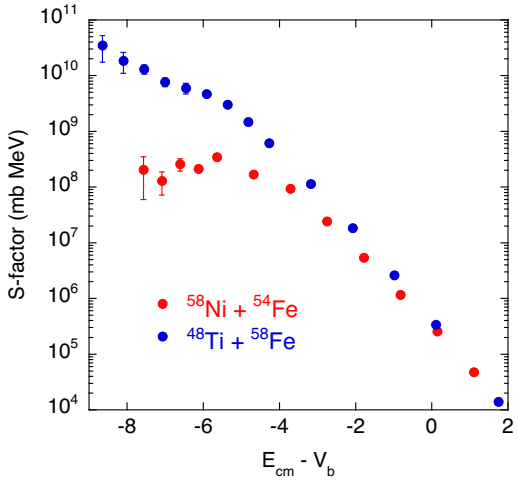

Figure 4. Astrophysical S factors for the two systems ^{48}Ti + ^{58}Fe and ^{58}Ni + ^{54}Fe vs. the energy difference from the Coulomb barrier. A clear maximum is observed for ^{58}Ni + ^{54}Fe only.

MeV, r_o= 1.13 fm and a = 0.67 fm, thus producing a barrier V_b = 75.0 MeV, i.e. 1.7 MeV higher than the nominal AW barrier (this brings some analogy to the situation found for ^{58}Ni + ^{54}Fe [12]).

One-phonon 2^+ and 3^- vibrations of projectile and target were included in the calculations. Since the quadrupole states of ^{48}Ti and ^{58}Fe are low in energy and rather strong (E_x= 0.984 and 0.811 MeV with β_2= 0.27 and 0.26, respectively), two-phonon excitations of this kind were included too. The corresponding octupole excitations are at E_x= 3.359 and 3.861 MeV with β_3= 0.27 and 0.18. The two-phonon excitations of this kind were not considered, because the effect of such high-energy octupole states (if existing) is included to a large extent in the adjustment of the ion-ion potential. All other possible mutual excitations have also been considered.

Fig. 2 (top) shows the calculated cross sections, together with the experimental data, in an energy scale relative to the barrier V_b = 75.0 MeV. The fit to the data is very good, and this can be even better appreciated in Fig. 3, where we report the logarithmic derivative (slope) of the excitation function compared to the data. L_{cs} is the slope expected for a constant astrophysical S factor. We have no indication of hindrance for ^{48}Ti + ^{58}Fe down to $\sigma_{fus} \simeq 1$ μb. We point out that the slope becomes rather flat (data and calculation) below ~ 67 MeV.

This is very different from the situation observed for the stiff system ^{58}Ni + ^{54}Fe. The analogous calculation shown in Fig. 2 (top) strongly overpredicts the cross sections below $\simeq$200 μb, as observed in the original paper [12]. The clear-cut difference between the sub-barrier behavior of the two system can be seen in Fig. 4. The nice S factor maximum that develops with decreasing energy for ^{58}Ni + ^{54}Fe, is not observed at all for ^{48}Ti + ^{58}Fe down to the lowest measured cross sections. The strong quadrupole modes of both ^{48}Ti and ^{58}Fe are likely to be responsible for this. It appears that the hindrance threshold is pushed to very low energies in the fusion of this system. Coupling to the two-neutron transfer channel which has a positive Q-value (+ 1.4 MeV) can also play a role. This will need further investigation.

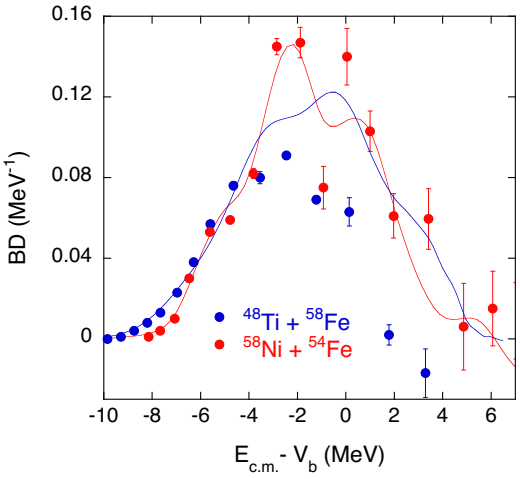

Figure 5. Barrier distributions obtained for the two systems vs. the energy difference from the Coulomb barrier. The lines are the distributions extracted from the CC calculations (see text).

We also compare the barrier distributions of the two systems in Fig. 5. They are plotted vs. the energy difference from the Coulomb barrier, so that they can be readily superimposed in the same plot. The distribution of ^{58}Ni + ^{54}Fe is wide, and has a complex structure with two main peaks having roughly equal weights (not completely separated) and a low-energy shoulder, as noted in Ref. [16]. This structure is well reproduced by the CC calculations shown by the red line taken from that article. The barrier distribution of ^{48}Ti + ^{58}Fe is not so wide, and it appears to be more structureless, as one would expect given the different nuclear structure of these two nuclei. It extends to lower energies with respect to ^{58}Ni + ^{54}Fe, and this obviously accounts for the larger cross sections of ^{48}Ti + ^{58}Fe well below the barrier (see Fig. 2). The present CC calculations (blue line) do not agree so well with the observed distribution. We stress again that the ^{48}Ti + ^{58}Fe data are preliminary ones, and this may particularly influence the barrier distribution whose extraction is very delicate, and strongly depends on the local trend of the excitation function. It appears anyway that the calculated distribution has too much "strength" from just below the barrier upwards.

4 Summary

Fusion cross sections for ^{48}Ti + ^{58}Fe have been measured from $\sigma_{fus} \simeq 1$ μb up to hundreds of mb . The fusion excitation function has been presented, and a significant irregularity of its logarithmic slope has been observed below the Coulomb barrier, but no evidence of hindrance shows up in the measured energy range. A comparison has been done with the near-by system ^{58}Ni + ^{54}Fe where the fusion hindrance appears at relatively high cross sections. The sub-barrier excitation function of ^{48}Ti + ^{58}Fe is much larger than what measured for ^{58}Ni + ^{54}Fe, where the slope increases steadily below the barrier. The fusion barrier distribution of ^{48}Ti + ^{58}Fe is rather wide, flat and structureless. The present new data for ^{48}Ti + ^{58}Fe can be reproduced by CC calculations using a Woods-Saxon potential, including the logarithmic derivative of the excitation function. The barrier distribution is not fit well by the calculations. It is suggested that the observed differences between the two systems are due to the stronger and lower-lying quadrupole modes of the two nuclei ^{48}Ti and ^{58}Fe.

The research leading to these results has received funding from the European Union 7th Framework Programme FP7/2007- 2013 under Grant Agreement No. 262010 - ENSAR. T.M. and S.S. were partially supported by the Croatian Ministry of Science, Education and Sports (Grant No. 0098-1191005-2890).

References

[1] Proc. Int. Conf. FUSION11. Saint-Malo, France, 2–6 May 2011, Eur. Phys. J. Web of Conferences **17**, 05001 (2011).
[2] M. Dasgupta, D.J.Hinde, N. Rowley and A. M. Stefanini, Annu. Rev. Nucl. Part. Sci. **48**, 401 (1998).
[3] H. Esbensen, Phys. Rev. C **72**, 054607 (2005).
[4] N. Rowley, G. R. Satchler and P. H. Stelson, Phys. Lett. B **254**, 25 (1991).
[5] A. M. Stefanini *et al.*, Phys. Rev. Lett. **74**, 864 (1995).
[6] C. L. Jiang *et al.*, Phys. Rev. Lett. **89**, 052701 (2002).
[7] M. Dasgupta, D. J. Hinde, A. Diaz-Torres, B. Bouriquet, Catherine I. Low, G. J. Milburn, and J. O. Newton, Phys. Rev. Lett. **99**, 192701 (2007).
[8] S. Misicu and H. Esbensen, Phys. Rev. Lett. **96**, 112701 (2006); Phys. Rev. C **75**, 034606 (2007).
[9] C. L. Jiang *et al.*, Phys. Rev. Lett. **93**, 012701 (2004).
[10] G. Montagnoli *et al.*, Phys. Rev. C **85**, 024607 (2012).
[11] A. M. Stefanini *et al.*, Phys. Rev. C **78**, 044607 (2008).
[12] A. M. Stefanini *et al.*, Phys. Rev. C **82**, 014614 (2010).
[13] G. Montagnoli *et al.*, Phys. Rev. C **87**, 014611 (2013).
[14] K. Hagino, N. Rowley and A. T. Kruppa, Comput. Phys. Commun. **123**, 143 (1999).
[15] Ö. Akyüz and Å. Winther, in Nuclear Structure and Heavy-Ion Physics, Proc. Int. School of Physics “E. Fermi", Course LXXVII, Varenna, eds. R. A. Broglia and R. A. Ricci (North Holland, Amsterdam, 1981).
[16] A. M. Stefanini *et al.*, Phys. Rev. C **81**, 037601 (2010).